

Temperature evolution of the Kondo peak beyond Fermi liquid theory

David Jacob^{1,2,*}

¹*Departamento de Polímeros y Materiales Avanzados: Física, Química y Tecnología, Universidad del País Vasco UPV/EHU, Av. Tolosa 72, E-20018 San Sebastián, Spain*

²*IKERBASQUE, Basque Foundation for Science, Plaza Euskadi 5, E-48009 Bilbao, Spain*

(Dated: October 24, 2023)

The limitation of Fermi liquid theory to very low energies and temperatures poses a fundamental problem for describing the temperature evolution of the Kondo peak. Here Fermi liquid theory for the single impurity Anderson model is extended beyond the low-energy and low-temperature regime by means of an ansatz for the impurity self-energy based on the accurate description of the Kondo peak by the Frota function, the similarity between energy and temperature in the second-order self-energy, and by exploiting Fermi liquid conditions. Analytic expressions for the temperature dependence of the Kondo peak height and width derived from this ansatz are in excellent agreement with numerical renormalization group data for temperatures beyond the Kondo temperature. The derived expression thus allows to unambiguously determine the intrinsic Kondo peak width and Kondo temperature from finite temperature measurements of the Kondo resonance.

Scanning tunneling microscopy (STM) has become an important experimental tool for studying magnetic atoms and molecules on metallic substrates [1–13]. In these systems the coupling of the atomic or molecular spin to the conduction electrons in the substrate can give rise to the Kondo effect [14]: the magnetic moment is screened due to formation of a total spin-singlet state between the atom or molecule and the conduction electrons. The Kondo effect is signaled by the appearance of a Kondo-Fano resonance in the STM spectra [15–19]. Therefore observation of the Kondo effect provides proof for magnetism in the uncoupled species [20, 21]. Together with the possibility to detect magnetic excitations via inelastic spin tunneling [6, 10, 22, 23], STM spectroscopy (STS) provides an excellent means for characterizing the magnetic properties of atoms, molecules and nanoclusters.

The Kondo temperature T_K is the energy scale that controls the low-temperature dynamics of a Kondo system [24]. Importantly, T_K defines a crossover temperature at which the system enters the Kondo regime and the Kondo peak starts to emerge. In STS, T_K is conveniently determined from the halfwidth Γ_K^0 of the Kondo peak, since $kT_K \sim \Gamma_K^0$ (see below for a more precise definition). However, STM spectra are often measured at temperatures comparable to T_K , where the Kondo peak is strongly broadened. In order to estimate the intrinsic (i.e. zero temperature) width of the Kondo peak, the temperature evolution of the Kondo peak width is recorded and extrapolated to zero temperature. This, however, requires knowledge about the functional form of the low-temperature evolution of the Kondo peak width [25].

Using results from Fermi liquid theory (FLT) [14, 26, 27], Nagaoka *et al.* derived a simple expression for the temperature dependence of the Kondo peak's halfwidth [28]: $\Gamma_{\text{NA}}(T) \sim \sqrt{2\tilde{\Delta}^2 + (\alpha kT)^2}$ where

$\alpha = \pi$ [4] and $\tilde{\Delta}$ is the renormalized width in FLT (see below) related to the Kondo temperature, $kT_K \sim \tilde{\Delta}$. This equation has been used in a number of papers to estimate the intrinsic width of the Kondo peak from finite temperature measurements [20, 21, 29–34]. However, in order to fit the experimental data, often the temperature coefficient α is used as an additional fit parameter, even though according to FLT α should be exactly π in the Kondo regime [14, 35]. The main problem is the limitation of FLT to very low temperatures and to very low energies (or bias voltages in STS) [36, 37]. For Kondo systems temperature and energy must be well below the Kondo temperature and width, effectively one order of magnitude below T_K . Especially the latter poses a fundamental problem, as it leads to a false estimate of the Kondo peak width even at zero temperature, see Fig. 1.

In order to overcome this problem, in this Letter FLT for Kondo systems will be extended to a larger range of energies and temperatures. Specifically, we focus on the single-impurity Anderson model (SIAM) [39]: a single impurity level of energy E_d subject to an on-site Coulomb repulsion U is coupled to a bath of non-interacting conduction electrons which gives rise to a constant broadening of the impurity with halfwidth Δ (wide band limit). Our starting point is the impurity Green's function (GF) for the particle-hole symmetric SIAM ($E_d = -U/2$) which according to renormalized perturbation theory (RPT) can be expressed in terms of renormalized quantities as [27]

$$G(\omega) = Z/[\omega + i\tilde{\Delta} - \tilde{\Sigma}(\omega; T)] \quad (1)$$

where the chemical potential μ has been set to zero. Z is the quasi-particle (QP) weight, $Z \equiv [1 - \partial_\omega \Sigma(0; 0)]^{-1}$ where $\Sigma(\omega; T)$ is the electronic self-energy resulting from the Coulomb repulsion U between electrons at the impurity site. $\tilde{\Delta} \equiv Z \cdot \Delta$ is the renormalized halfwidth of the impurity level, and $\tilde{\Sigma}(\omega; T) \equiv Z(\Sigma(\omega; T) - \Sigma(0; 0) - \omega \partial_\omega \Sigma(0; 0))$ is the *renormalized* self-energy, describing interaction effects between QPs. Note that at particle-

* david.jacob@ehu.es

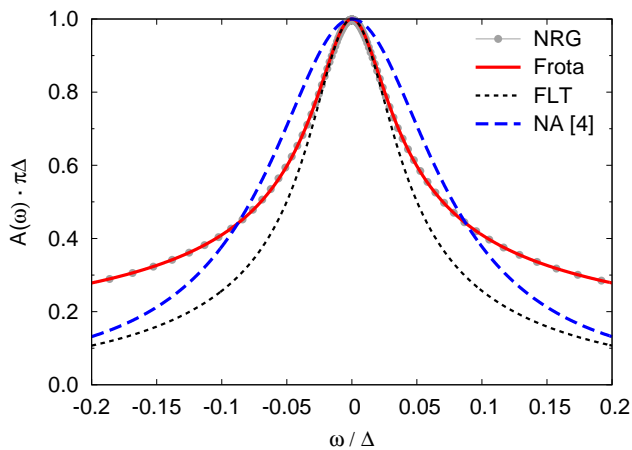


FIG. 1. SFs for the SIAM with $U = -2E_d = 10\Delta$ at $T = 0$ calculated by NRG (gray full circles) [38] compared to the approximate SFs given by FLT (black dashed line) and NA [4] (blue dashed line). Also shown is the Frota lineshape (red solid line) fitted to the NRG data with Δ_K as the fitting parameter ($\Delta_K \sim 0.0275 \cdot \Delta$) and the amplitude given by Friedel sum rule, $A_K^0 = 1/\pi\Delta$. The QP weight entering the FLT and NA expressions for the SFs is $Z \sim 0.055$, obtained from the curvature of the NRG SF at the Fermi level.

hole symmetry the Hartree contribution to the self-energy $\Sigma(0, 0) = U/2$ exactly cancels $E_d = -U/2$ in the denominator of the GF; also by construction $\tilde{\Sigma}(0; 0) = \partial_\omega \tilde{\Sigma}(0; 0) = 0$. From the GF we can determine the spectral function (SF), $A(\omega; T) = -\text{Im} G(\omega; T)/\pi$, which can be directly related to the dI/dV spectra in STS [40, 41].

Perturbation theory to second order [42] yields for the renormalized self-energy $\tilde{\Sigma}_2(\omega; T) = -i[\omega^2 + (\pi kT)^2]/2\tilde{\Delta}$. Hence to second order the SF in FLT is given by $A_{\text{FLT}}(\omega; T) = -\frac{1}{\pi} \text{Im}(Z/\{\omega + i\tilde{\Delta}[1 + \frac{1}{2}(\omega/\tilde{\Delta})^2 + \frac{1}{2}(\pi kT/\tilde{\Delta})^2]\})$. By making a further approximation to the FLT SF [43] Nagaoka *et al.* obtained a Lorentzian form for the SF [4], i.e. $A_{\text{NA}}(\omega; T) = \frac{1}{\pi\tilde{\Delta}}[(\omega/2\tilde{\Delta})^2 + 1 + (\pi kT/2\tilde{\Delta})^2]^{-1}$ with halfwidth given by $\Gamma_{\text{NA}}(T)$.

Figure 1 shows the Kondo peak in the SF computed by numerical renormalization group (NRG) [38] compared to the approximate SFs $A_{\text{FLT}}(\omega)$ and $A_{\text{NA}}(\omega)$ for $T = 0$, where the QP weight Z has been obtained by matching the *curvatures* of A_{FLT} at $T = 0$ and the actual Kondo peak in the NRG SF at the Fermi level, i.e., $\partial_\omega^2 A_{\text{FLT}}(0; 0) = \partial_\omega^2 A(0; 0)$. In FLT the halfwidth of the actual Kondo peak Γ_K^0 is considerably underestimated, even though the fit with the actual Kondo peak at low energies $\omega \ll \Gamma_K^0$ is perfect. In contrast, the Nagaoka approximation (NA) for the SF considerably overestimates the halfwidth. Additionally, the NA SF does not correctly capture the curvature of the Kondo peak at the Fermi level either. Thus while the FLT SF yields a proper low-energy and low-temperature description of the Kondo peak, the NA actually does not.

The underestimate of the Kondo peak width in A_{FLT}

is owed to the low-energy nature of FLT, limiting the validity of the SFs to energies $\omega \ll \Gamma_K^0$. The same problem arises for the temperature dependence which is likewise limited to very low temperatures $T \ll T_K \sim \Gamma_K^0$. In principle this problem could be solved by including higher order terms in the perturbation expansion. However, very high order terms would be required to achieve a meaningful extension of the energy and temperature range of FLT. But with growing order the terms also become increasingly cumbersome for an analytical treatment [44, 45].

On the other hand, the Frota function $A_F(\omega) = A_K^0 \cdot \text{Re}\sqrt{i\Delta_K/(\omega + i\Delta_K)}$ [46] yields an essentially exact description of the Kondo peak for energies up to several times the halfwidth Γ_K^0 , as shown by the red curve in Fig. 1. A_K^0 is the amplitude of the Frota function, while Δ_K determines its halfwidth via $\Gamma_K^0 = \sqrt{3 + \sqrt{12}} \cdot \Delta_K = 2.542 \cdot \Delta_K$. It is now important to realize that the parameters for the Frota function can be determined *exactly* from FLT since FLT becomes exact in the limit $\omega \rightarrow 0, T \rightarrow 0$. First, Friedel sum rule determines the amplitude of the Kondo peak, resulting in $A_K^0 = 1/\pi\Delta$. Second, matching the curvatures of the Frota SF and FLT SF at the Fermi level, $\partial_\omega^2 A_F(0) = \partial_\omega^2 A_{\text{FLT}}(0; 0)$, yields $\Delta_K = \tilde{\Delta}/2 = Z \cdot \Delta/2$. This is how Z in Fig. 1 was determined in practice: instead of taking the second derivative of the NRG spectral function numerically, which tends to be very noisy, first the Frota lineshape was determined via the Δ_K parameter, and then the QP weight via $Z = 2\Delta_K/\Delta$.

Additionally, the finding $\Delta_K = \tilde{\Delta}/2$ allows us to establish an *exact* relation between the Kondo temperature T_K according to Wilson [24] and the intrinsic width of the Kondo peak Γ_K^0 . According to FLT $\pi\tilde{\Delta} = 4kT_K/w$ where $w = 0.4128$ is Wilson's number [14], hence $\Delta_K = 2kT_K/\pi w \sim 1.542kT_K$, and therefore:

$$\Gamma_K^0 = 2.542 \Delta_K = \frac{2.542 \times 2}{\pi \cdot w} kT_K \sim 3.92 kT_K \quad (2)$$

The prefactor of 3.92 is close to the value of ~ 3.7 found numerically by Zitko and Pruschke from NRG calculations [47].

We next determine the renormalized self-energy $\tilde{\Sigma}$ that exactly yields the Frota lineshape at $T = 0$. First, we introduce the ‘‘Frota GF’’ whose imaginary part yields the Frota spectral function, $G_F(\omega) \equiv -\frac{i}{\tilde{\Delta}} \sqrt{i\Delta_K/(\omega + i\Delta_K)}$, where $\Delta_K = \tilde{\Delta}/2$. The corresponding renormalized self-energy that yields $G_F(\omega)$ when plugged into (1) is easily determined to be $\Sigma_F(\omega) = \omega + i2\Delta_K \left(1 - \sqrt{1 - i\omega/\Delta_K}\right)$.

The crucial step now is to extend the $T = 0$ ‘‘Frota self-energy’’ Σ_F to finite temperatures. Inspired by the symmetry in ω and πkT of the second order contribution to the self-energy $\tilde{\Sigma}_2 \sim i[\omega^2 + (\pi kT)^2]$, we make the following Ansatz for the temperature-dependent $\tilde{\Sigma}$:

$$\tilde{\Sigma}(\omega; T) = \text{Re} \Sigma_F(\omega) + i \text{Im} \Sigma_F[\varepsilon(\omega; T)] \quad (3)$$

where $\varepsilon(\omega; T) \equiv \sqrt{\omega^2 + (\pi kT)^2}$. Note that the real part of $\tilde{\Sigma}$ is crucial to recover the Frota lineshape at $T = 0$.

The real and imaginary parts of $\tilde{\Sigma}$ can be written explicitly as real functions:

$$\text{Re } \tilde{\Sigma}(\omega; T) = \omega - \sigma_\omega \sqrt{2} \Delta_K \sqrt{S(\omega/\Delta_K) - 1} \quad (4)$$

$$\text{Im } \tilde{\Sigma}(\omega; T) = 2 \Delta_K - \sqrt{2} \Delta_K \sqrt{S(\varepsilon/\Delta_K) + 1} \quad (5)$$

where $\sigma_\omega \equiv \text{sgn}(\omega)$ is the sign function and $S(x) \equiv \sqrt{1+x^2}$ has been introduced. The GF can now be written as:

$$G(\omega; T) = \frac{\sqrt{2}/\Delta}{\sigma_\omega \sqrt{S\left(\frac{\omega}{\Delta_K}\right) - 1 + i\sqrt{S\left(\frac{\varepsilon(\omega, T)}{\Delta_K}\right) + 1}} \quad (6)$$

In the limit $T \rightarrow 0$ the GF reduces to the Frota form, given by $G_F(\omega)$. In the following we concentrate on the spectral function [48] given by the imaginary part of (6) which can be written as

$$A(\omega; T) = \frac{\sqrt{2}}{\pi \Delta} \frac{\sqrt{S\left(\frac{\varepsilon(\omega, T)}{\Delta_K}\right) + 1}}{S\left(\frac{\omega}{\Delta_K}\right) + S\left(\frac{\varepsilon(\omega, T)}{\Delta_K}\right)} \quad (7)$$

A first test for the validity of the Ansatz (3) for the temperature dependent $\tilde{\Sigma}$ is to compute the temperature dependent height of the Kondo peak, found by evaluating A at $\omega = 0$:

$$A_0(T) = \frac{1}{\pi \Delta} \sqrt{\frac{2}{1 + \sqrt{1 + \left(\frac{\pi kT}{\Delta_K}\right)^2}}} \quad (8)$$

Figure 2(a) shows the height $A_0(T)$ according to (8) compared to NRG data [49], and to the height computed within FLT or NA (both approximations coincide for $\omega = 0$). The agreement between (8) and NRG is excellent for temperatures up to T_K , and very good for temperatures up to the bare linewidth, $kT \lesssim \Delta$. In contrast, in FLT (or NA) the decay of the SF with temperature is far too strong, leading to a severe underestimate of the Kondo peak height already for temperatures $\sim T_K$.

Next we determine the halfwidth of the Kondo peak Γ_K as a function of temperature, which can be obtained from the condition $A(\Gamma_K; T) = \frac{1}{2} A_0(T)$. Inserting Eqs. (7) and (8) and squaring yields:

$$S(\varepsilon/\Delta_K) + 1 = \frac{1}{4} \frac{[S(\Gamma_K/\Delta_K) + S(\varepsilon/\Delta_K)]^2}{1 + S(\pi kT/\Delta_K)} \quad (9)$$

Using the identity $[S(\varepsilon/\Delta_K)]^2 = [S(\Gamma_K/\Delta_K)]^2 + (\pi kT/\Delta_K)^2$ in Eq. (9) would lead to a quartic equation for $S(\Gamma_K/\Delta_K)$, which could in principle be solved analytically, but leads to a very long and cumbersome expression for $S(\Gamma_K/\Delta_K)$. Instead we Taylor expand $S(\varepsilon/\Delta_K) \approx S(\Gamma_K/\Delta_K) + (\pi kT/\Delta_K)^2/2S(\Gamma_K/\Delta_K)$,

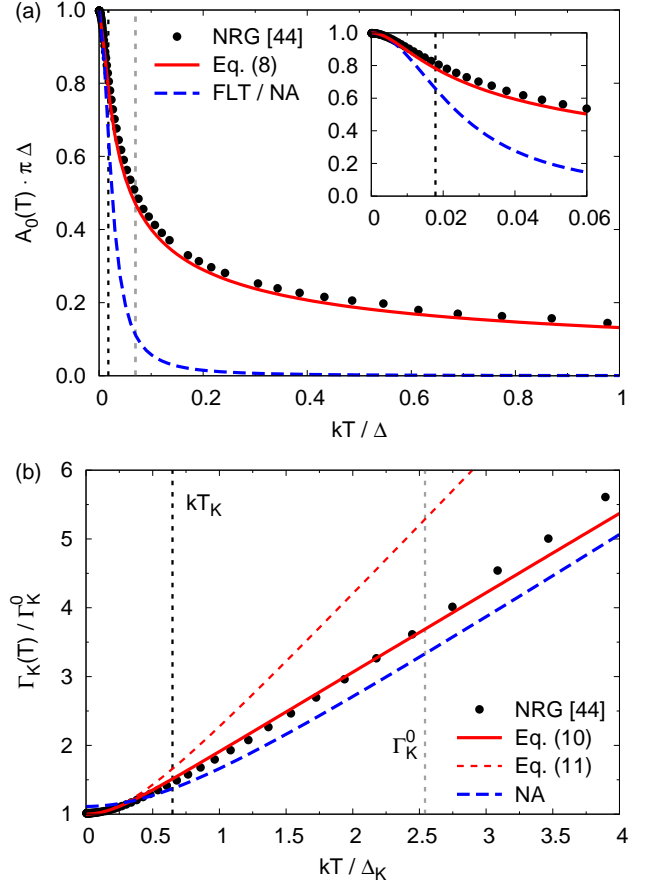


FIG. 2. Height and halfwidth of Kondo peak as functions of temperature T for the SIAM with $U = -2E_d = 10\Delta$. (a) Height $A_0(T)$ according to (8) (full red line), compared to NRG (black circles) [38, 49], and to the height computed within FLT or NA (both approximations coincide for $\omega = 0$). The inset shows a close-up of the low-temperature region. (b) Halfwidth $\Gamma_K(T)$ according to (10) (full red line), compared to NRG (black circles) [38, 49], and to the NA given by $\Gamma_{NA}(T)$ (blue dashed line) [4]. The thin red dashed line shows the low-temperature approximation (11). The vertical black and gray dashed lines show $kT_K = \Delta_K/1.542 \sim 0.018 \Delta$ and $\Gamma_K^0 = 2.542 \Delta_K \sim 0.070 \Delta$, respectively. The same QP weight as in Fig. 1, $Z \sim 0.055$, has been used.

leading to $[S(\Gamma_K/\Delta_K) + S(\varepsilon/\Delta_K)]^2 \approx 4S(\Gamma_K/\Delta_K)^2 + 2(\pi kT/\Delta_K)^2$. This approximation leads to a biquadratic equation for $S(\Gamma_K/\Delta_K)$ which can be solved easily. Using $\Gamma_K = \Delta_K \sqrt{S^2 - 1}$, we finally obtain the halfwidth of the Kondo peak as a function of temperature [50]:

$$\Gamma_K(T) = \Delta_K \cdot \sqrt{a + b \sqrt{1 + \left(\frac{\pi kT}{\Delta_K}\right)^2} + c \left(\frac{\pi kT}{\Delta_K}\right)^2} \quad (10)$$

where $a \equiv 1 + \sqrt{3} \sim 2.732$, $b \equiv 2 + \sqrt{3} \sim 3.732$, and $c \equiv \sqrt{3}/2 \sim 0.866$ are constants, and the Frota width parameter Δ_K yields the Kondo temperature $T_K = \Delta_K/1.542$ and the intrinsic halfwidth $\Gamma_K^0 = 2.542 \Delta_K$.

Equation (10) is the central result of this paper. As shown in Fig. 2(b), it is in excellent agreement with NRG data for temperatures up to T_K , and is very accurate for temperatures up to $\Gamma_K^0/k \sim 2.542 \Delta_K/k$ where it starts to deviate more strongly from NRG. In contrast, the temperature evolution of the Kondo peak width in the NA given by $\Gamma_{NA}(T)$ [Eq. (8) of Ref. 4] yields a poor description of the NRG data in the entire temperature range. The curvature in the NA in the temperature range $kT \leq \Delta_K$ is very different both from the NRG data and from $\Gamma_K(T)$ given by Eq. (10). It also leads to an overestimate of $\sim 10\%$ for the intrinsic Kondo peak width in agreement with Fig. 1.

Taylor expansion of the inner square root in (10) to second order, $\sqrt{1 + (\pi kT/\Delta_K)^2} \approx 1 + \frac{1}{2}(\pi kT/\Delta_K)^2$, yields an approximate expression for the halfwidth that resembles the expression found by Nagaoka *et al.* [4]:

$$\Gamma_K(T) \approx \sqrt{(\Gamma_K^0)^2 + (\alpha kT)^2} \quad (11)$$

where now $\alpha = \sqrt{1 + \sqrt{3}} \cdot \pi \sim 5.193$, different from π found by Nagaoka *et al.*, but also different from the values found by fitting α in the NA to experimental data for spin-1/2 Kondo systems [21, 31, 34]. Note that Eq. (11) is only valid in the very low temperature regime $T \ll T_K$, as shown by the red dashed line in Fig. 2(b), which starts to deviate considerably from the exact result (10) for $kT \gtrsim 0.3\Delta_K \sim 0.5T_K$. However, experimental STS data is usually measured at temperatures comparable to T_K , where the approximation (11) is not accurate anymore, explaining fit values of α different from 5.193. Recently, it was also pointed out that simple square root expressions can in general not capture the correct behavior of Kondo linewidth both in the low and high-temperature regime [37].

Finally, we test how well Eq. (10) can be fitted to existing STS data of a spin-1/2 Kondo system. Figure 3 shows the temperature evolution of the Kondo halfwidth for the fused Goblet dimer deposited on Au(111), measured by STS [34] (black solid squares) compared to fits of the halfwidth $\Gamma_K(T)$ given by Eq. (10) (red solid line) and to $\Gamma_{NA}(T)$ in the NA (blue dashed line). While Eq. (10) performs somewhat better than the NA, it obviously does not fit very well the experimental data either, even though the temperatures are well below $\Gamma_K^0/k \sim 37\text{K}$ [34], where Eq. (10) is expected to be very accurate according to the comparison with NRG, c.f. Fig. 2(b).

A likely explanation for the disagreement is the presence of additional broadening mechanisms in the STS experiment, often not taken into account in the analysis of the STS data, as recently discussed by Gruber *et al.* [33]. For example, smearing of the Fermi-Dirac (FD) distribution at the STM tip leads to temperature-dependent broadening of the dI/dV spectra, described by a convolution of the derivative of the FD distribution and the spectral function [33, 37], which can be evaluated numerically. The intrinsic halfwidth of the Kondo peak in the underlying spectral function can then be deter-

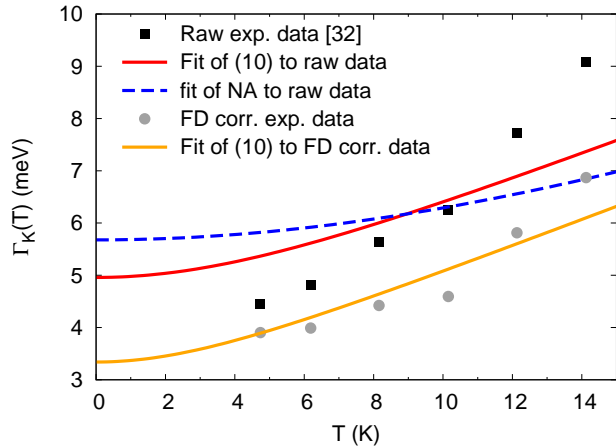


FIG. 3. Measured halfwidth of the Kondo peak versus temperature (black solid squares) and fit to $\Gamma_K(T)$ given by (10) (full red line) for the fused Goblet dimer (data from Ref. 34), resulting in $\Delta_K \sim 1.95\text{meV}$ corresponding to $\Gamma_K^0 \sim 5.0\text{meV}$ and $T_K \sim 15\text{K}$. The blue dashed line shows a fit to the halfwidth $\Gamma_{NA}(T)$ in the NA. FD corrected halfwidths [51] are shown as solid gray circles, while the full orange line shows a fit of $\Gamma_K(T)$ given by (10) to these, resulting in $\Delta_K \sim 1.3\text{meV}$ corresponding to $\Gamma_K^0 \sim 3.3$ and $T_K \sim 9.9\text{K}$.

mined by numerically solving the equation for the effective halfwidth of the Kondo peak in the dI/dV [51]. The gray circles in Fig. 3 show the thus FD corrected experimental data. For the experimental temperature range the effect of FD broadening is considerable (20% – 30%). As shown by the orange line in Fig. 3, the FD correction leads to a considerably better fit of Eq. (10) with the data. Importantly, it leads to a considerably lower estimate of Γ_K^0 and T_K . Also other broadening mechanisms discussed in Ref. 33 may play a role, and further improve the fit, when taken into account. The issue of accurately measuring Kondo widths in STS experiments clearly deserves further attention.

In summary, the Fermi liquid description of the Kondo peak has been extended to a larger energy and temperature range by means of an ansatz for the temperature dependent renormalized self-energy. The extension beyond Fermi liquid theory is crucial to correctly describe the width of the Kondo peak at finite temperatures. Analytic expressions derived from this ansatz for the height and width of the Kondo peak at finite temperatures show excellent agreement with numerical renormalization group data up to experimentally relevant temperatures around T_K . The derived expression for the temperature evolution of the Kondo peak width thus allows to extract the intrinsic Kondo peak width and corresponding Kondo temperature from finite-temperature STS measurements of Kondo systems. The discrepancy with published experimental STS data of a spin-1/2 Kondo system [34] can certainly be attributed to the neglect of extrinsic broadening mechanisms in the analysis of the STS data.

ACKNOWLEDGMENTS

I am grateful to Elia Turco, Nils Krane, Pascal Ruffieux, Roman Fasel, Somesh Ganguli, Markus Aapro, Robert Drost, and Peter Liljeroth for fruitful discussions. I would also like to thank Rok Žitko for providing me with the NRG data of Ref. 49, reading of the manuscript

and for useful comments. I am further grateful to Stefan Kurth and Joaquín Fernández-Rossier who also read the manuscript and provided useful comments. This work was financially supported by Grant PID2020-112811GB-I00 funded by MCIN/AEI/10.13039/501100011033 and by Grant No. IT1453-22 from the Basque Government.

-
- [1] V. Madhavan, W. Chen, T. Jamneala, M. F. Crommie, and N. S. Wingreen, *Science* **280**, 567 (1998).
- [2] J. Li, W.-D. Schneider, R. Berndt, and B. Delley, *Phys. Rev. Lett.* **80**, 2893 (1998).
- [3] H. C. Manoharan, C. P. Lutz, and D. M. Eigler, *Nature* **403**, 512 (2000).
- [4] K. Nagaoka, T. Jamneala, M. Grobis, and M. F. Crommie, *Phys. Rev. Lett.* **88**, 077205 (2002).
- [5] N. Knorr, M. A. Schneider, L. Diekhöner, P. Wahl, and K. Kern, *Phys. Rev. Lett.* **88**, 096804 (2002).
- [6] A. J. Heinrich, J. A. Gupta, C. P. Lutz, and D. M. Eigler, *Science* **306**, 466 (2004).
- [7] A. Zhao, Q. Li, L. Chen, H. Xiang, W. Wang, S. Pan, B. Wang, X. Xiao, J. Yang, J. G. Hou, and Q. Zhu, *Science* **309**, 1542 (2005).
- [8] P. Wahl, P. Simon, L. Diekhöner, V. S. Stepanyuk, P. Bruno, M. A. Schneider, and K. Kern, *Phys. Rev. Lett.* **98**, 056601 (2007).
- [9] V. Iancu, A. Deshpande, and S.-W. Hla, *Nano Lett.* **6**, 820 (2006).
- [10] C. F. Hirjibehedin, C.-Y. Lin, A. F. Otte, M. Ternes, C. P. Lutz, B. A. Jones, and A. J. Heinrich, *Science* **317**, 1199–1203 (2007).
- [11] A. F. Otte, M. Ternes, K. von Bergmann, S. Loth, H. Brune, C. P. Lutz, C. F. Hirjibehedin, and A. J. Heinrich, *Nat. Phys.* **4**, 847 (2008).
- [12] J. C. Oberg, M. R. Calvo, F. Delgado, M. Moro-Lagares, D. Serrate, D. Jacob, J. Fernández-Rossier, and C. F. Hirjibehedin, *Nat. Nanotechnol.* **9**, 64 (2014).
- [13] S. Karan, D. Jacob, M. Karolak, C. Hamann, Y. Wang, A. Weismann, A. I. Lichtenstein, and R. Berndt, *Phys. Rev. Lett.* **115**, 016802 (2015).
- [14] A. C. Hewson, *The Kondo problem to heavy fermions* (Cambr. Univ. Press, Cambridge, 1997).
- [15] O. Újsághy, J. Kroha, L. Szunyogh, and A. Zawadowski, *Phys. Rev. Lett.* **85**, 2557 (2000).
- [16] A. Schiller and S. Hershfield, *Phys. Rev. B* **61**, 9036 (2000).
- [17] V. Madhavan, W. Chen, T. Jamneala, M. F. Crommie, and N. S. Wingreen, *Phys. Rev. B* **64**, 165412 (2001).
- [18] P. P. Baruselli, R. Requist, A. Smogunov, M. Fabrizio, and E. Tosatti, *Phys. Rev. B* **92**, 045119 (2015).
- [19] S. Frank and D. Jacob, *Phys. Rev. B* **92**, 235127 (2015).
- [20] J. Li, S. Sanz, J. Castro-Esteban, M. Vilas-Varela, N. Friedrich, T. Frederiksen, D. Peña, and J. I. Pascual, *Phys. Rev. Lett.* **124**, 177201 (2020).
- [21] E. Turco, A. Bernhardt, N. Krane, L. Valenta, R. Fasel, M. Juríček, and P. Ruffieux, *JACS Au* **3**, 1358 (2023).
- [22] J. Fernández-Rossier, *Phys. Rev. Lett.* **102**, 256802 (2009).
- [23] R. Žitko and T. Pruschke, *New. J. Phys.* **12**, 063040 (2010).
- [24] Here we use Wilson’s thermodynamic definition of T_K [52] corrected by Wiegman and Tsvetlick [53], i.e., $\chi(T_K)/(g\mu_B)^2 = 0.0704/kT_K$ where $\chi(T)$ is the magnetic susceptibility, g the electronic g-factor, and μ_B the Bohr magneton.
- [25] An alternative route for determining T_K from STS at $T \sim T_K$ was recently proposed in Ref. 54. This approach, however, requires additional control parameters in the experiment such as a magnetic field or mechanical gating which may not always be available.
- [26] P. Nozières, *J. Low Temp. Phys.* **17**, 31 (1974).
- [27] A. C. Hewson, *Phys. Rev. Lett.* **70**, 4007 (1993).
- [28] In the paper by Nagaoka *et al.* actually the equivalent equation for the full width is reported.
- [29] A. Zhao, Z. Hu, B. Wang, X. Xiao, J. Yang, and J. G. Hou, *The Journal of Chemical Physics* **128**, 234705 (2008).
- [30] S. Ernst, S. Kirchner, C. Krellner, C. Geibel, G. Zwicknagl, F. Steglich, and S. Wirth, *Nature* **474**, 362 (2011).
- [31] Y.-h. Zhang, S. Kahle, T. Herden, C. Stroh, M. Mayor, U. Schlickum, M. Ternes, P. Wahl, and K. Kern, *Nature Communications* **4**, 2110 (2013).
- [32] A. A. Khajetoorians, M. Valentyuk, M. Steinbrecher, T. Schlenk, A. Shick, J. Kolorenc, A. I. Lichtenstein, T. O. Wehling, R. Wiesendanger, and J. Wiebe, *Nature Nanotechnology* **10**, 958 (2015).
- [33] M. Gruber, A. Weismann, and R. Berndt, *Journal of Physics: Condensed Matter* **30**, 424001 (2018).
- [34] S. Mishra, D. Beyer, K. Eimre, S. Kezilebieke, R. Berger, O. Gröning, C. A. Pignedoli, K. Müllen, P. Liljeroth, P. Ruffieux, *et al.*, *Nat. Nanotechnol.* **15**, 22 (2019).
- [35] T. A. Costi, A. C. Hewson, and V. Zlatic, *J. Phys. Condens. Mat.* **6**, 2519 (1994).
- [36] C. Chen, I. Sodemann, and P. A. Lee, *Phys. Rev. B* **103**, 085128 (2021).
- [37] See Supplementary Note 12 of Ref. 55.
- [38] NRG data were provided by R. Žitko and correspond to the spectra shown in Fig. 21 of Ref. 49, computed via the Padé approximant approach.
- [39] P. W. Anderson, *Phys. Rev.* **124**, 41 (1961).
- [40] D. Jacob and S. Kurth, *Nano Lett.* **18**, 2086 (2018).
- [41] D. Jacob, *Journal of Physics: Condensed Matter* **30**, 354003 (2018).
- [42] K. Yamada, *Progress of Theoretical Physics* **53**, 970 (1975).
- [43] The approximation essentially consists in neglecting the energy dependence in the denominator of the GF (1) outside the renormalized self-energy, i.e., $G_2(\omega) \approx G_{NA}(\omega) \equiv Z/[i\tilde{\Delta} - \tilde{\Sigma}_2(\omega; T)]$.
- [44] F. Lesage and H. Saleur, *Phys. Rev. Lett.* **82**, 4540 (1999).
- [45] A. C. Hewson, *J. Phys. Condens. Mat.* **13**, 10011 (2001).
- [46] H. O. Frota, *Phys. Rev. B* **45**, 1096 (1992).

- [47] R. Žitko and T. Pruschke, Phys. Rev. B **79**, 085106 (2009).
- [48] The GF (6) only approximately satisfies Kramers-Kronig relations for $T > 0$. However, only its imaginary part is of interest here, so that the moderate inconsistency with the real part is not a problem. See the Supplemental Material for details.
- [49] Ž. Osolin and R. Žitko, Phys. Rev. B **87**, 245135 (2013).
- [50] See Supplemental Material for details of the proof.
- [51] See Supplemental Material for details of the numeric correction scheme.
- [52] K. G. Wilson, Rev. Mod. Phys. **47**, 773 (1975).
- [53] P. B. Wiegmann and A. M. Tselick, Journal of Physics C: Solid State Physics **16**, 2281 (1983).
- [54] M. Žonda, O. Stetsovych, R. Korytár, M. Ternes, R. Temirov, A. Raccanelli, F. S. Tautz, P. Jelínek, T. Novotný, and M. Švec, The Journal of Physical Chemistry Letters **12**, 6320 (2021).
- [55] C. van Efferen, J. Fischer, T. A. Costi, A. Rosch, T. Michely, and W. Jolie, Modulated Kondo screening along magnetic mirror twin boundaries in monolayer MoS2 on graphene (2023), arXiv:2210.09675.

Supplemental Material: Accurate temperature evolution of the Kondo peak beyond Fermi liquid theory

David Jacob^{1,2,*}

¹*Departamento de Polímeros y Materiales Avanzados: Física, Química y Tecnología, Universidad del País Vasco UPV/EHU, Av. Tolosa 72, E-20018 San Sebastián, Spain*

²*IKERBASQUE, Basque Foundation for Science, Plaza Euskadi 5, E-48009 Bilbao, Spain*

I. DERIVATION OF EQ. (10) FROM EQ. (9) IN MAIN TEXT

We introduce the abbreviations $S_\varepsilon \equiv S(\varepsilon/\Delta_K)$, $S_\Gamma \equiv S(\Gamma_K/\Delta_K)$, $\tau \equiv \pi kT/\Delta_K$ and $S_\tau \equiv S(\tau)$, where $S(x) = \sqrt{1+x^2}$ as defined in the main text after Eq. (6). Eq. (9) of the main text then becomes

$$S_\varepsilon + 1 = \frac{1}{4} \frac{(S_\Gamma + S_\varepsilon)^2}{1 + S_\tau} \quad (\text{S1})$$

Using $S_\varepsilon^2 = S_\Gamma^2 + \tau^2$ we can rewrite the numerator of the r.h.s. of (S1) as

$$(S_\Gamma + S_\varepsilon)^2 = S_\Gamma^2 + 2 S_\Gamma S_\varepsilon + S_\varepsilon^2 = 2 S_\Gamma^2 + \tau^2 + 2 S_\Gamma S_\varepsilon \quad (\text{S2})$$

For $\tau < S_\Gamma$ we can Taylor expand S_ε as $S_\varepsilon = \sqrt{S_\Gamma^2 + \tau^2} \approx S_\Gamma + \frac{\tau^2}{2S_\Gamma}$. Hence the numerator of the r.h.s. of (S1) can be approximated by

$$(S_\Gamma + S_\varepsilon)^2 \approx 4S_\Gamma^2 + 2\tau^2 \text{ for } \tau \ll S_\Gamma \quad (\text{S3})$$

Eq. (S1) then becomes

$$\sqrt{S_\Gamma^2 + \tau^2} \approx \frac{1}{4} \frac{4S_\Gamma^2 + 2\tau^2}{1 + S_\tau} - 1 \quad (\text{S4})$$

Squaring both sides and reorganizing the terms yields a bi-quadratic equation for S_Γ :

$$(S_\Gamma^2)^2 + p(\tau) S_\Gamma^2 + q(\tau) = 0 \quad (\text{S5})$$

where

$$p(\tau) = -4(1 + S_\tau) < 0 \quad \text{and} \quad q(\tau) = -\frac{3}{4}S_\tau^4 - 3S_\tau^3 - \frac{1}{2}S_\tau^2 + 5S_\tau + 4 - \frac{3}{4} \quad (\text{S6})$$

Solving for S_Γ^2 yields the solution

$$S_\Gamma^2 = -\frac{p(\tau)}{2} + \sqrt{\left(\frac{p(\tau)}{2}\right)^2 - q(\tau)} \quad (\text{S7})$$

where the positive sign has been chosen in order to guarantee $S_\Gamma^2 > 0$ for all τ . The expression under the square root can be simplified to yield:

$$\left(\frac{p(\tau)}{2}\right)^2 - q(\tau) = \frac{3}{4} + 3S_\tau + \frac{9}{2}S_\tau^2 + 3S_\tau^3 + \frac{3}{4}S_\tau^4 = \frac{3}{4} (1 + S_\tau)^4 \quad (\text{S8})$$

Plugging this into Eq. (S7) and solving for $\Gamma_K = \Delta_K \sqrt{S_\Gamma^2 - 1}$ we obtain the following equation for the halfwidth of the Kondo peak as a function of the temperature:

$$\Gamma_K(T) = \Delta_K \cdot \sqrt{1 + 2 S_\tau + \sqrt{\frac{3}{4} (1 + S_\tau)^2}} \quad (\text{S9})$$

Using $S_\tau = \sqrt{1 + \tau^2} = \sqrt{1 + \left(\frac{\pi kT}{\Delta_K}\right)^2}$ and reorganizing the terms, we obtain Eq. (10) of the main text.

* david.jacob@ehu.es

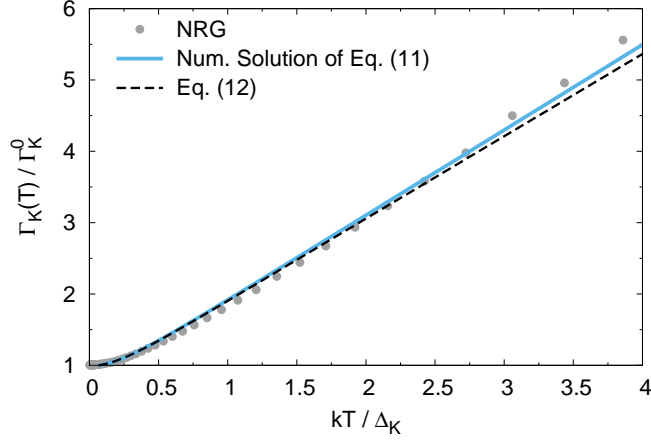


FIG. S1. Numeric solution of Eq.(9) compared to the approximate analytic solution (10) in the main text and to NRG data for the same Anderson model parameters as in Figs. 1-3 in the main text. (NRG data are courtesy of R. Žitko and correspond to spectra shown in Fig. 21 of Ref. 1.)

II. COMPARISON OF EQ. (10) WITH EXACT NUMERICAL SOLUTION OF EQ. (9) IN MAIN TEXT

The approximate analytic solution (10) can be benchmarked by direct numerical solution of Eq. (9) or (S1), respectively. To this end $S_\varepsilon^2 = S_\Gamma^2 + \tau^2$ is substituted everywhere in (S1), leading to

$$\sqrt{S_\Gamma^2 + \tau^2} + 1 - \frac{1}{4} \frac{(S_\Gamma + \sqrt{S_\Gamma^2 + \tau^2})^2}{1 + S_\Gamma} = 0 \quad (\text{S10})$$

which can be solved numerically for the root S_Γ at each temperature $\tau \equiv \pi kT / \Delta_K$ using, e.g., the bisection method. The halfwidth is then obtained from $\Gamma_K = \Delta_K \sqrt{S_\Gamma^2 - 1}$. Fig. S1 shows the numeric solution of Eq. (9) compared to $\Gamma_K(T)$ given by Eq. (10) and to the NRG data. Evidently the analytic expression (10) in the main text yields an excellent approximation to the exact numeric solution of Eq. (9) in the relevant temperature range $kT \leq \Gamma_K^0 = 2.542\Delta_K$.

III. FERMI-DIRAC BROADENING

At finite temperature T at the STM tip the differential conductance of the current I from the tip to the molecule at the surface is given by [2, 3]:

$$\mathcal{G}(V; T, \Gamma_K) \equiv \frac{d\tilde{I}}{dV} \propto \int d\omega [-f'(\omega)] A(\omega + eV; \Gamma_K) \quad (\text{S11})$$

where $f'(\omega)$ is the derivative of the Fermi-Dirac (FD) distribution $f(\omega) = 1/[1 + \exp(\beta\omega)]$, $A(\omega; \Gamma_K)$ is the spectral function of the molecule, $\beta = 1/kT$, V is the applied bias voltage, and Γ_K is the actual width of the Kondo peak in the underlying spectral function $A(\omega; \Gamma_K)$, that we wish to determine. The convolution (S11) can be evaluated numerically. Approximating the spectral function with a Frota lineshape $A(\omega; \Gamma_K) \sim \text{Re} \left[1/\sqrt{1 + i\omega \cdot 2.542/\Gamma_K} \right]$, we can obtain the actual halfwidth Γ_K of the Kondo peak in the spectral function at temperature T as the root of the function

$$g(x) \equiv \mathcal{G}(\tilde{\Gamma}(T)/e; T, x) - \frac{1}{2}\mathcal{G}(0; T, x) \quad (\text{S12})$$

where $\tilde{\Gamma}(T)$ is the measured halfwidth of the Kondo feature as seen in the dI/dV at temperature T (including FD broadening). The root $g(x) \stackrel{!}{=} 0$ is found numerically using the bisection algorithm, and corresponds to the actual halfwidth of the Kondo peak corrected for the FD broadening at temperature T , $\Gamma_K \equiv x$. The FD corrected halfwidths are shown as grey circles for each measured temperature T in Fig. 3 in the main text.

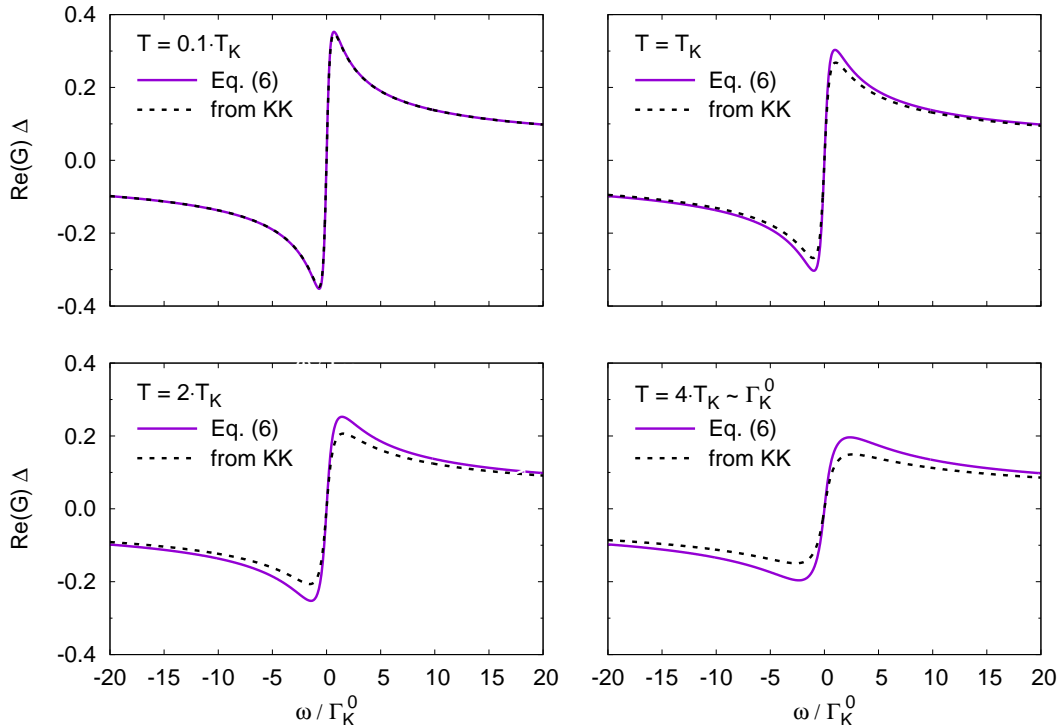


FIG. S2. Comparison of real part of GF given by Eq. (6) in main text and real part obtained from imaginary part of GF by numerical evaluation of Kramers-Kronig relation (S13) for different temperatures.

IV. KRAMERS-KRONIG RELATIONS

As mentioned in footnote [48] of the main text the GF (6) obtained from the Ansatz only approximately fulfills Kramers-Kronig relations for $T > 0$. Fig. S2 shows a comparison between the real part of the GF obtained from (6) and the real part obtained from a numerical evaluation of the Kramers-Kronig relation

$$\text{Re}[G(\omega)] = \frac{1}{\pi} P \int d\omega' \frac{\text{Im}[G(\omega' + i\eta)]}{\omega' + i\eta - \omega} \quad (\text{S13})$$

where $i\eta$ is a small imaginary part added in order to avoid the pole at $\omega' = \omega$. For $T = 0$ the GF (6) recovers the Frota form for which Kramers-Kronig is exactly fulfilled. Also for very small temperatures $T \ll T_K$ the agreement is excellent. For temperatures up to T_K the discrepancy is still very small. Only for higher temperatures $T > 2 \cdot T_K$ the discrepancy becomes appreciable. In any case for the purpose of the paper the slight inconsistency between real part and imaginary part of the GF is not of importance, since for the derivation of width and height of the Kondo peak only the imaginary part or spectral function is of interest.

[1] Ž. Osolin and R. Žitko, Phys. Rev. B **87**, 245135 (2013).

[2] D. Jacob and S. Kurth, Nano Lett. **18**, 2086 (2018).

[3] M. Gruber, A. Weismann, and R. Berndt, Journal of Physics: Condensed Matter **30**, 424001 (2018).